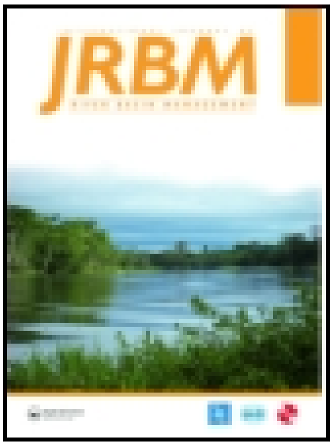

International Journal of River Basin Management
Publication details, including instructions for authors and subscription information:
http://www.tandfonline.com/loi/trbm20

Modelling the time variance of the river bed roughness coefficient for improved simulation of water levels

Ingrid Keupers[a], Thuy Nguyen Thanh[b] & Patrick Willems[c]

[a] PhD student, Department of Civil Engineering, Hydraulics section, KU Leuven, Leuven, Belgium.

[b] PhD student, Department of Civil Engineering, Hydraulics section, KU Leuven, Leuven, Belgium. Email:

[c] Professor, Department of Civil Engineering, Hydraulics section, KU Leuven, Leuven, Belgium. Email:

Published online: 11 Feb 2015.

Intl. J. River Basin Management, 2015, 1–12

Research paper

Modelling the time variance of the river bed roughness coefficient for improved simulation of water levels

INGRID KEUPERS, *PhD student, Department of Civil Engineering, Hydraulics section, KU Leuven, Leuven, Belgium. Email: ingrid.keupers@bwk.kuleuven.be (author for correspondence)*

THUY NGUYEN THANH, *PhD student, Department of Civil Engineering, Hydraulics section, KU Leuven, Leuven, Belgium. Email: thuy.nguyenthanh@bwk.kuleuven.be*

PATRICK WILLEMS, *Professor, Department of Civil Engineering, Hydraulics section, KU Leuven, Leuven, Belgium. Email: patrick.willems@bwk.kuleuven.be*

ABSTRACT

Aquatic macrophytes create seasonally variable changes in river bed roughness. These changes in roughness influence the hydrodynamic behaviour of the river, for example, elevated water levels for the same discharge. In most hydrodynamic river models, the roughness is assumed constant in time, which may lead to high errors in the river water level results. When the river water level results are applied to water quality studies, biased estimates may be obtained of river flow velocities, dilution and other water quality processes. This article investigates how models implemented in two common hydrodynamic modelling software packages (MIKE11 and InfoWorks RS) can be adopted to take into account the time-varying river bed roughness due to plant growth. Albeit the use of a different approach by the two models, it is shown that both can account for that influence. After application to the Grote Nete river catchment in Belgium, far more accurate river water level results are obtained. Overall, the increase in accuracy of the water level simulations outweighs the increase in model complexity required to enable simulation of the vegetation changes. The model results can also be used to correct discharge estimates based on the measured water levels as shown for this case study.

Keywords: InfoWorks RS; MIKE11; plant growth; rating curve; roughness coefficient; water level prediction

1 Introduction

1.1 *Background and objectives*

Rating curves developed from water level and discharge measurements at flow measuring stations are used by agencies and researchers worldwide to monitor the flow along rivers. These measurements typically assume that discharge–water level relationships are stable over time. Where evidence exists for a non-stationary relationship, rating curves or estimated flows are adjusted, or shifted, based upon field measurements. An understanding of the nature and rate of change in the discharge–water level relationships is therefore important for the proper management of river systems, particularly when dealing with the management of water quality, aquatic habitat and water supply.

The drivers of the discharge–water level relationships along rivers are the river bed roughness, slope and cross-section geometry. The roughness is a very important driver, but most often estimated based on expert judgement, hence rather subjectively. In addition to long-term changes in discharge–water level relationships, for example, due to morphological riverbed changes, some rivers have high seasonal variation caused by growth of aquatic macrophytes. Growth of aquatic macrophytes is a known, common source of seasonal variability in flow resistance (Watson 1987; Bakry *et al.* 1992; Gurnell and Midgley 1994; Barnett and Shamseldin 2009; King 2011). The effect of aquatic macrophytes on discharge–water level relationships is potentially large in small rivers and streams, creating significant errors in flow estimates and water level simulations. Hydrodynamic river studies nevertheless often assume the roughness coefficient to be constant, hence disregarding the effect of vegetation growth. For water quality studies, this may lead to biased estimates of river flow velocities, dilution and other water quality processes. Where high

Received on 13 May 2014. Accepted on 11 November 2014.

ISSN 1571-5124 print/ISSN 1814-2060 online
http://dx.doi.org/10.1080/15715124.2014.999782
http://www.tandfonline.com

nutrient loadings are present in rivers with low velocities, aquatic macrophytes can grow abundantly and possibly mitigate the detrimental effects of this pollution stress. Indeed, a lower velocity means longer residence time and higher sedimentation rates and thus a higher self-purifying capacity (Schulz *et al.* 2003).

Despite the importance of the effect of seasonal river bed vegetation change on discharge estimation, it is not commonly studied in contrast to the effect of vegetation on the flow and water levels in floodplains, which has received ample attention (Anderson *et al.* 2006; Straatsma *et al.* 2013). Studies that did focus on the effect of vegetation on in-channel flow mainly focused on intensive measurements campaigns to determine the type and extent of the vegetation cover (Bakry *et al.* 1992; Green 2006; De Doncker *et al.* 2011; Pham *et al.* 2011). However, such detailed measurement campaigns cannot be always conducted, thus giving rise to the need for a modelling framework that uses the widely available water level measurements to account for the seasonal variation of the river bed roughness.

This need has also been addressed by Aricò *et al.* (2009, 2010), where discharge and channel roughness are estimated simultaneously based on water level measurements at different sections along the river. In many cases, however, the density of water level gauging stations is rather low such that seldom more than one station is available along a river reach.

Based on a case study in Belgium, this article investigates how two commonly applied full hydrodynamic modelling packages, MIKE11 and InfoWorks RS, can incorporate the effect of a seasonally changing roughness coefficient due to vegetation growth. The models are calibrated against measured water levels. The difference in approach to be applied for both model codes is explored and the effect of this divergence on the water level simulation results is investigated. Secondly, it is studied if the changed roughness due to vegetation is dependent on the magnitude of the discharge. Indeed, it has been shown previously that river vegetation responds dynamically to increased flow velocity, with the streamlining of leaves reducing the effective drag coefficient of the water plants (Arcement and Schneider 1984; Järvelä 2002; Green 2005; Wilson 2007; De Doncker *et al.* 2011). If it is found that the roughness due to vegetation is diminished during high flow conditions, this dependence of course needs to be taken into account for river flood modelling as to not overestimate the occurrence and extent of flooding. Finally, it is shown how the calibrated hydrodynamic model can be used to correct the discharge–water level relationships seasonally such that it can be used directly to estimate the discharge from the water level measurements.

1.2 *Study area*

The study area is the Grote Nete catchment, located in the northeast of Belgium (Figure 1). The catchment has a total area of 386 km^2 and is flat, with an average slope of 3‰. The total length of the water courses is 539 km, equivalent to a drainage density of 1.4 km/km^2. The Grote Nete catchment was chosen because of the abundant growth of aquatic macrophytes during the summer season in most of the rivers, as is the case for many small streams in the rural areas of northern Belgium because of high nutrient loadings by agricultural activities.

The Grote Nete catchment experiences moderate average winter (October until March) and summer (April to September) temperatures of 5°C and 14°C, respectively. The average winter and summer precipitations are, respectively, 372 and 392 mm, giving a long-term mean annual precipitation equal to 764 mm. The average annual potential evapotranspiration is 670 mm (Woldeamlak *et al.* 2007). Because the soil type predominantly consists of sandy and loamy sand, rainfall easily percolates to the groundwater resulting in a shallow water table. The groundwater therefore has a large influence on the flow characteristics. Seasonal groundwater fluctuations determine the flow profile with a daily mean discharge of 3.6 m^3 s^{-1} during summer and a higher mean discharge of 5.7 m^3 s^{-1} during winter at the basin outlet. Peak discharges can reach up to 15 m^3 s^{-1} during winter (Wijns and Wilkin 2007).

2 General methodology

2.1 *Hydrologic rainfall–runoff model*

An important component of any hydrodynamic river model is the catchment rainfall–runoff model. For this case study, the VHM (Vereenvoudigd Hydrologisch Model) approach developed by Willems (2014) is used. This approach is based on a step-wise procedure to determine (identify and calibrate) the

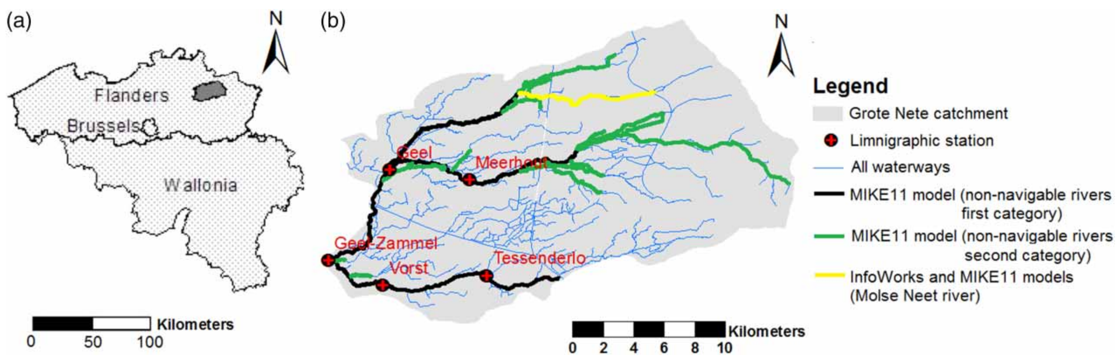

Figure 1 Location of the Grote Nete catchment in Belgium (a); close-up of this catchment (b).

equations that control the split of the catchment rainfall input in the contributions to the different hydrological subflows (overland flow, subsurface runoff and baseflow) and the soil water storage (which is emptied by evapotranspiration). Catchment routing of the subflows is done by means of calibrated conceptual reservoirs to determine the magnitude of the runoff subflows, which are added together to determine the total catchment rainfall runoff.

2.2 *Hydrodynamic river model*

Both the MIKE 11 hydrodynamic (HD) and InfoWorks RS modelling systems compute 1D HD unsteady flows along rivers. They solve the vertically integrated equations of conservation of volume (Eq. 1) and momentum (Eq. 2) also known as the 'Saint Venant' equations.

$$\frac{\delta Q}{\delta x} + \frac{\delta A}{\delta t} = q_{\mathrm{lat}}, \tag{1}$$

$$\frac{\delta Q}{\delta t} + \frac{\delta}{\delta x}\left(\frac{\alpha Q^2}{A}\right) + gA\left(\frac{\delta h}{\delta x} - S_0\right) + g\frac{AQ|Q|}{K^2} = 0, \tag{2}$$

where Q is the discharge (m^3 s^{-1}), x is the streamwise direction (m), A is the wetted cross-section area (m^2), t is the time (s), q_{lat} is the lateral inflow (m^3 s^{-1}), α is the momentum correction coefficient (–), g is the gravitational acceleration (m s^{-2}), h is the surface water level (m), S_0 is the longitudinal bed slope (m/m) and K is the conveyance (m^3 s^{-1}).

The first term of the momentum equation is called the local acceleration term, the second term, the convective term, the third term, the pressure term and the last term, the source/gravity term. It is this last term that causes the water to flow. How much water can flow through the river is quantified by the conveyance capacity, K, of the river. The ability of a channel to convey water directly influences the water levels as resistance to flow results in smaller velocities and greater depths. The conveyance capacity of the river depends on channel morphology, that is, cross-section shape and planform sinuosity and the roughness characteristics of the river bed.

2.2.1 *MIKE11 model*

In MIKE11, the model grid is discretized in time and space so that the differential Saint Venant equations can be solved by the six-point implicit difference scheme developed by Abbott and Ionescu (1967). The roughness can be described by three different roughness coefficients in MIKE 11 namely the Chezy, Manning or Darcy–Weisbach formulation. In this study, it was chosen to model the roughness by using the Manning coefficient, n. The conveyance can be calculated based on this Manning coefficient using Eq. 3. The value of n is typically in the range from 0.01 s m$^{-1/3}$ (smooth channel) to 0.10 s m$^{-1/3}$ (thickly vegetated channel) (DHI 2011). A global value can be imposed, or different values can be set for particular rivers or river reaches. It is not possible to define a time-varying roughness coefficient. However, a global or distributed boundary can be imposed that introduces a resistance factor (r_{f}) time series to specified river reaches. At each time step, r_{f} is multiplied by the resistance number, thus effectively making the roughness coefficient a function of time. It is not possible to directly take into account the effect that time-varying flow magnitude may have on the vegetation and resistance. This effect can be incorporated, but only indirectly, if the rainfall–runoff model and the hydrodynamic model are run offline. The temporal flow magnitude variations can be determined from the result of the rainfall–runoff model, from which the relative resistance factors can be calculated. These factors can then be used in the hydrodynamic simulation to obtain correct water level estimates.

$$K = \frac{A \cdot R^{2/3}}{n}, \tag{3}$$

$$R_{\mathrm{h}} = \left(\frac{\Sigma_{i=1}^{N}\left(\frac{A_i^{5/3}}{r_{\mathrm{r},i} \cdot p_i^{2/3}}\right)}{A}\right)^{3/2}, \tag{4}$$

$$\sqrt{R_*} = 1\Big/\sum_{i=1}^{N}\left(\frac{A_i}{r_{\mathrm{r},i}}\right) \cdot \int_0^B \frac{H^{3/2}}{r_{\mathrm{r}}}\,\mathrm{d}b, \tag{5}$$

where P is the wetted perimeter (m), n is the Manning coefficient (s m$^{-1/3}$), R_{h} is the hydraulic radius (m), N is the number of subsections (–), $r_{\mathrm{r},i}$ is the relative resistance for sub-section i, H is the local water depth normal to the bed (m) and B is the water width at the same elevation (m)

The conveyance, K, can be calculated based on the roughness coefficient n by using either the hydraulic radius (Eq. 4) or the resistance radius formulation (Eq. 5). If the relative resistance is constant across the whole cross-section, Eq. 4 simplifies to dividing the wet cross-section area by the wet perimeter. If the resistance radius is applied, the conveyance may be overestimated, especially for narrow channels as its formulation does not fully take into account the friction from the cross-section sides as does the formulation for the hydraulic radius. For both radius types, verification is required for each cross-section on the conveyance relationship which has to be monotonously increasing with increasing water level, as this is one of the key assumptions for open water hydraulics. A non-monotonous relationship could be obtained when there is a sudden increase in width in the section geometry (DHI 2011).

2.2.2 *InfoWorks RS model*

In InfoWorks RS, the differential Saint Venant equations for the discretized model grid are solved by a four-point implicit difference scheme developed by Preissmann (1961). Two different options are available in InfoWorks RS to estimate the conveyance: the Manning approach which is also adopted in MIKE11 and the Reynolds-Averaged Navier–Stokes (RANS) approach. The first approach does not allow a time-varying Manning coefficient and cannot therefore be adopted in the light of this research. The second approach uses a Depth-integration of the RANS equations for flow in the streamwise direction. The Shiono and Knight form of the depth-averaged momentum equation for application to channel flow is given in Eq. 6. The first term represents the variation in hydrostatic pressure along the reach, the second term the boundary friction effects, the third term the turbulence due to shearing between the lateral layers and the right-hand term, the turbulence due to secondary currents (DEFRA/EA 2002).

$$\begin{aligned} &gHS_0 - \frac{f\beta q^2}{gH^2} + \frac{\partial}{\partial y}\left[\lambda H\left(\frac{f}{g}\right)^{1/2} q\frac{\partial}{\partial y}\left(\frac{q}{H}\right)\right] = \frac{1.1-\sigma}{0.1}\Gamma \\ &\quad + \frac{\sigma-1.0}{0.1}C_{uv}\frac{\partial}{\partial y}\left[\frac{q^2}{H}\right] \quad \text{if} \quad 1.0 \le \sigma \le 1.1 \\ &gHS_0 - \frac{f\beta q^2}{gH^2} + \frac{\partial}{\partial y}\left[\lambda H\left(\frac{f}{g}\right)^{1/2} q\frac{\partial}{\partial y}\left(\frac{q}{H}\right)\right] \\ &= C_{uv}\frac{\partial}{\partial y}\left[\frac{q^2}{H}\right] \quad \text{if} \quad \sigma > 1.1, \end{aligned} \tag{6}$$

where q is the streamwise unit flow rate (m^2 s^{-1}), y is the lateral distance across section (m), β is the coefficient for the influence of lateral bedslope on the bed shear stress (–), f is the bed friction factor (–), λ is the dimensionless eddy viscosity (–), Γ is the secondary flow term, σ is the sinuosity (m/m) and C_{uv} is the coefficient that relates the secondary currents to the depth mean velocity (–).

The unit roughness n_l represents the local roughness for an identifiable segment of boundary friction within the channel section. The local roughness is calculated based on three components that are user defined namely bed, bank or floodplain surface material, vegetation and irregularities (Eq. 7). The 'root sum of the squares' approach highlights the contribution of the largest roughness component. The roughness is squared before being combined since the energy loss is related to the square of the local velocity.

$$n_l = [n_{sur}^2 + n_{veg}^2 + n_{irr}^2]^{1/2}, \tag{7}$$

where n_l is the total unit roughness (s m$^{-1/3}$) , n_{sur} is the unit roughness value due to surface material (s m$^{-1/3}$), n_{veg} is the unit roughness value due to vegetation (s m$^{-1/3}$) and n_{irr} is the unit roughness value due to irregularity (s m$^{-1/3}$).

The Colebrook–White equation (Eq. 8) is selected in preference to the Manning equation in the RANS approach, as (i) it covers smooth, transitional and rough flow conditions; (ii) it has a strong physical basis as it is derived from the logarithmic velocity profile together with the channel geometry; and (iii) it incorporates the roughness variation with depth. The roughness height k_s is therefore calculated from the local roughness (Eq. 9) (DEFRA/EA 2002).

$$\frac{1}{\sqrt{f}} = -2.01\ \log\left[\frac{k_s}{12.40H} + \frac{3.02q}{4\theta\sqrt{f}}\right], \tag{8}$$

$$n_l = 0.038\, k_s^{1/6}, \tag{9}$$

where k_s is the absolute roughness height (m) and ϑ is the kinematic viscosity (m^2 s^{-1})

The roughness magnitude is equivalent to a Manning's n that has been stripped of all the energy losses due to lateral shear, secondary flows and sinuosity. In other words, Manning's n represents overall cross-section resistance. To clarify the difference between these two methods, the Manning's n is back calculated after applying RANS to estimate the conveyance by the Manning equation (Eq. 10)

$$n = \frac{AP^{2/3}S^{1/2}}{Q}, \tag{10}$$

where n is the back calculated Manning's n (s m$^{-1/3}$), S is the energy slope (m/m) and Q is the flow (m^3 s^{-1}).

Equation 6 has five parameters that can be calibrated namely (i) the local boundary friction factor f, (ii) the dimensionless eddy viscosity λ, (iii) the secondary flow term Γ, (iv) the sinuosity σ and (v) the coefficient that relates the secondary currents to the depth mean velocity C_{uv}. Since the local boundary friction value f is calculated based on the unit roughness value n_l, the value of λ is calculated from the main channel eddy viscosity λ_{mc} (Abril 2003), Γ is fixed in the hard code of the InfoWorks RS software and C_{uv} is determined by the sinuosity of the channel σ (Ervine *et al.* 2000), only three parameters remain that can be calibrated to get a good estimation of the conveyance and hence the water height namely n_l, λ_{mc} and σ. Of these parameters, only the vegetation component of the local roughness parameters can vary in time. For readability, the total local roughness input in the model is shown hereafter instead of the three separate components and is referred to as the roughness coefficient n_l.

3. Specific application methodology to the study area

3.1 *Hydrologic rainfall–runoff model*

A lumped VHM model has been implemented for the Grote Nete catchment, based on rainfall and evapotranspiration time series as input. The average areal rainfall is calculated with the Thiessen polygon method based on six rain gauges with hourly measurements for the years 2004–2007. For the same period, daily measurements performed by the KMI/IRM (Royal Meteorological Institute of Belgium) at Uccle were considered for the evapotranspiration input. The VHM model was calibrated by

Vansteenkiste *et al.* (2014) for the period 2003–2005 and validated for 2006–2008 and applied in this study without modifications.

3.2 *Hydrodynamic river model*

3.2.1 *MIKE11 model*

The MIKE11 hydrodynamic model that has been set up for the Grote Nete case study includes the three main river branches of the catchment, namely the Molse Nete, the Grote Nete and the Grote Laak, and its main tributaries, which together cover a total river length of 139 km (Figure 1). The Grote Nete River is regulated by several gated weirs to maintain minimum river water levels during low flow periods and for flood control during peal flow periods. The Grote Laak and the Molse Nete Rivers are less regulated, but pass through many civil structures such as bridges and culverts. All these man-made structures are implemented in the MIKE11 model to ensure accurate simulation of water levels. Detailed river topographical data were available with cross-sections every 50 metres on average, and at shorter distances close to the structures that require a higher space resolution. This high space resolution requires a small simulation time step (Δt 30 seconds) to avoid numerical instability. The hydraulic radius formulation was used because of the presence of many narrow sections. The model has been set up in previous studies (Keupers and Willems 2013; Vansteenkiste *et al.* 2014).

There are five limnigraphic stations situated in the Grote Nete catchment. Of these, the Meerhout measuring station shows the largest influence of vegetation growth on the water level during summer months. These measurements are therefore used for calibration of the Manning's n. This calibration was done by minimizing the root mean squared error (RMSE) or difference between simulated and observed water depths. The population simplex evolution method was applied with the goal to reach global optimum values for the Manning coefficient during the specified period. The initial values for n were set by Monte Carlo sampling and n was allowed to vary from 0.01 to 0.2 s m$^{-1/3}$. The calibration procedure was repeated each five days during the calibration period 2004–2006, each time with a two-day warm-up period. The warm-up periods were discarded from the error calculation. The year 2007 was used for validation. In this way, daily varying roughness coefficients were obtained, to be applied to all river branches in the model.

3.2.2 *InfoWorks RS model*

For one of the river branches in the Grote Nete catchment, the Molse Neet river, next to the MIKE11 model, also an InfoWorks RS model has been implemented (Figure 1). The same structures and cross-sectional data were implemented as in the MIKE11 model. A small simulation time step of five seconds was required to ensure stability of the model.

Because there is no limnigraphic station along the Molse Neet River (Figure 1), it was not possible to calibrate the river bed roughness model in InfoWorks RS with observed water levels. Instead, the MIKE11 simulation results at distance 8.034 km along the Molse Neet river branch are used for that calibration. In this way, the implication of the difference in implementation of the time-varying roughness coefficient between both software packages could be studied.

To avoid overfitting, a local sensitivity analysis was first implemented to determine the most sensitive parameter(s). Parameter n_l was identified as more sensitive than the other parameters λ_{mc} and σ. Therefore, only n_l was calibrated, whereas for λ_{mc} and σ, recommend values for straight rivers ($\lambda_{mc} = 0.24$, $\sigma = 1.00$; DEFRA/EA 2002) were considered. The time-varying roughness coefficient n_l was determined as for the MIKE11 model, by minimizing the RMSE in water depths, but this time based on the differences in simulation results of MIKE11 and InfoWorks RS. The initial roughness values selected for the optimization were calibrated roughness values in MIKE11 (see previous section). After calibration for the period 2004–2005, validation was done for the period 2006–2007.

4 Results and discussion

4.1 *MIKE11 calibration roughness coefficient*

First, the hydrodynamic simulation is performed with a constant value of the Manning coefficient equal to 0.035 s m$^{-1/3}$ as is common practice for this study area (Figure 2). It is clear that a constant roughness coefficient is insufficient for this case study as overestimations of the water depths occur during the winter months and underestimations during the summer periods. This is also shown by the very low Nash–Sutcliffe Efficiency (NSE; Nash and Sutcliffe 1970) of 0.31 when simulated and observed water levels are compared for the whole period (January 2004 to December 2007).

After calibration based on the water level observations for 2004–2006, Manning's n values range from 0.014 to 0.156 s m$^{-1/3}$. This range is consistent with the range reported by the Danish Hydraulic Institute (DHI 2011), the measured Manning coefficients recorded by Bakry *et al.* (1992), the calibrated Manning coefficients reported by Aronica *et al.* (1998) and the theoretical Manning coefficients noted in Green (2005). From October till May, the values fluctuate around 0.03 s m$^{-1/3}$. When in May the aquatic macrophytes start to grow, the roughness strongly increases to reach a peak in August after which a quick decrease is observed to the value for a river bed with little vegetation. The top panel of Figure 3 shows the calibrated n values together with the RMSE after calibration. When this value was larger than 0.005 m for some periods, it was considered non-reliable, hence disregarded when analysing the temporal variations. Finally, a piecewise

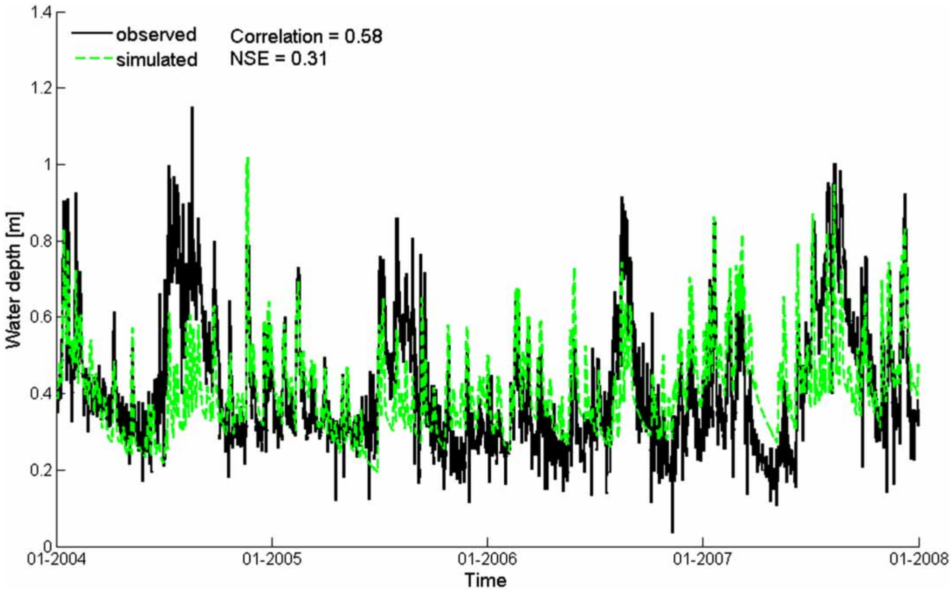

Figure 2 Observed versus MIKE11 simulated water depths at Meerhout, after use of a constant Manning coefficient of 0.035 s m$^{-1/3}$.

linear relationship of Manning coefficient versus day of the year could be distilled as shown in the bottom panel of Figure 3.

After simulation of the daily changing Manning coefficient in MIKE11 (Figure 4), the NSE increases from 0.31 for the whole period to 0.68 in the calibration period (2004–2006) and 0.65 in the validation period (2007), indicating a much higher accuracy in simulated water levels. This is also shown in Figure 5 as water depths simulated with a time-varying roughness coefficient approach the cumulative probability function of the observed water depths much closer than water depths that are simulated with a constant roughness coefficient. Especially the lower water depths are simulated well, whereas the probability of higher water depths is slightly overestimated for the calibration period. For the validation period, this overestimation is much larger.

When investigating the results for the summer of 2007, it becomes clear that there are many high peak flow events during this summer and that water levels are overestimated (Figure 6). This indicates diminished roughness during such high flow periods as compared to the base roughness. Hence, it can be concluded that the roughness coefficient depends on the river discharge next to the season or vegetation state. The

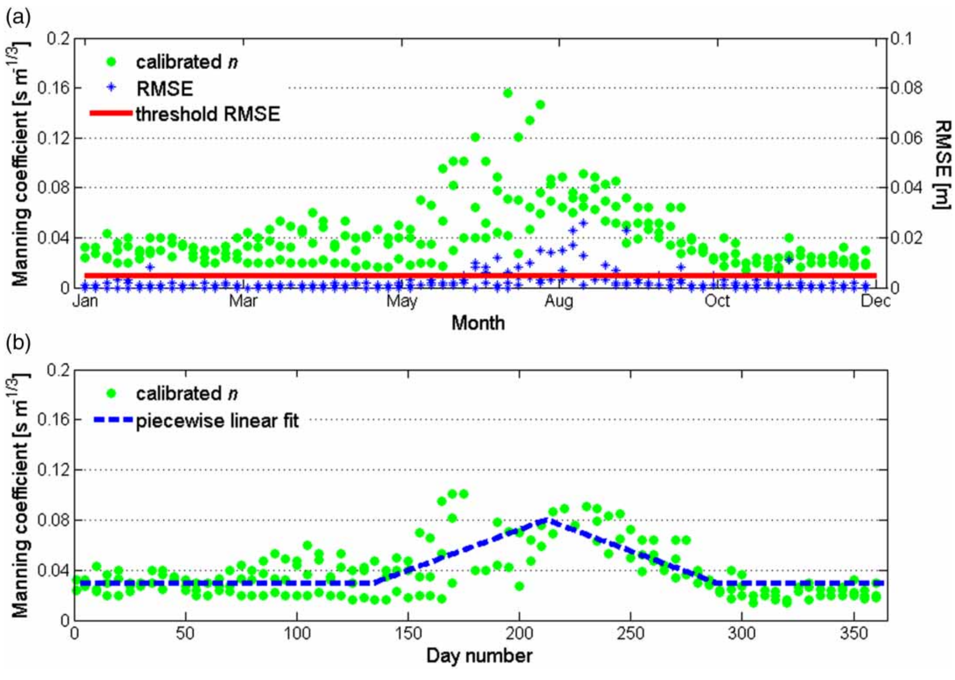

Figure 3 Calibrated Manning's *n* values per five-day period with RMSE for calibrated value (a) and piecewise linear relation of the Manning's *n* versus day of the year (b).

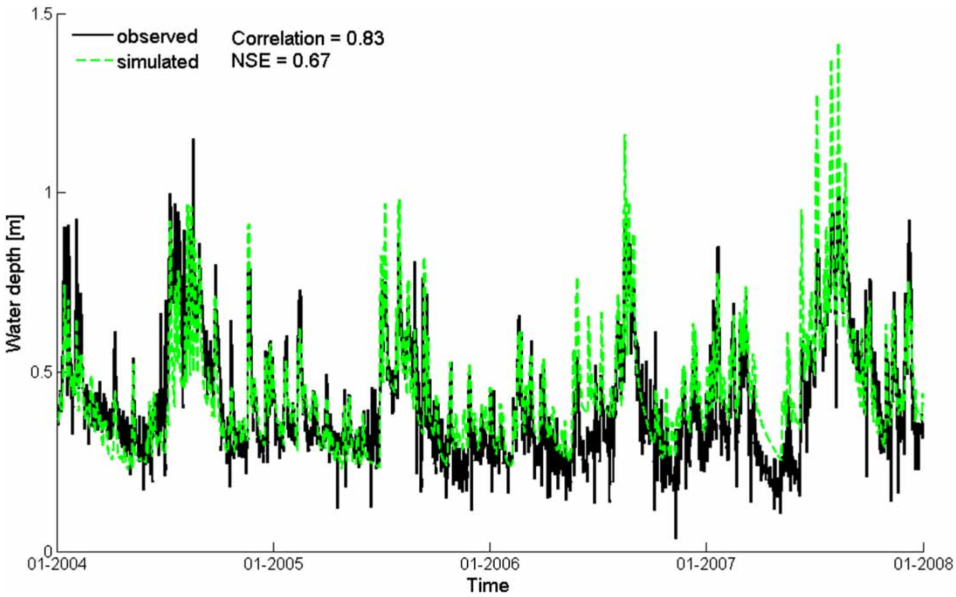

Figure 4 Observed versus MIKE11 simulated water depths at Meerhout, afters use of a time-varying Manning coefficient.

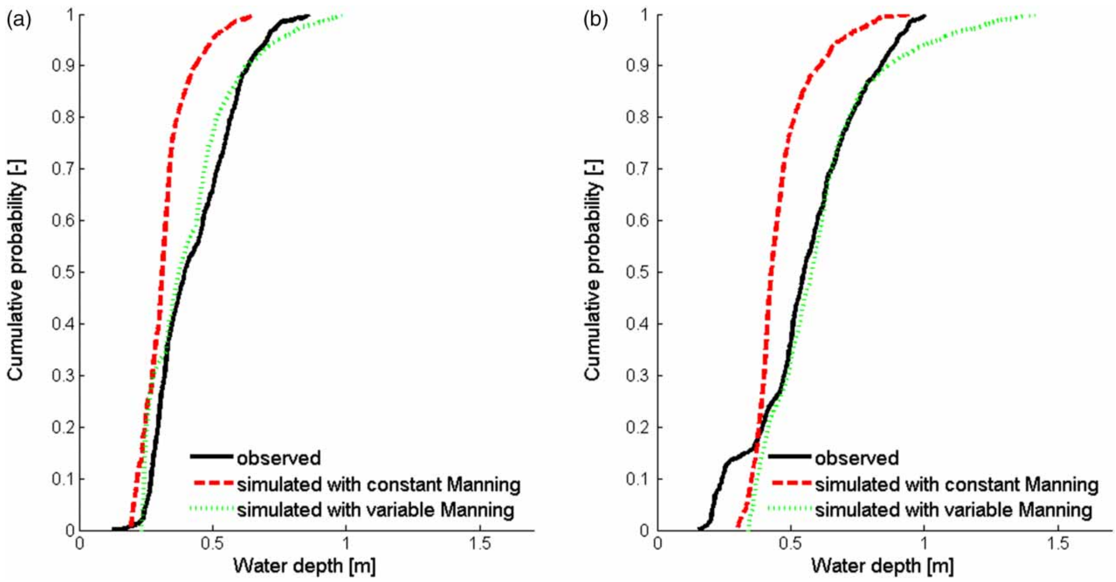

Figure 5 Cumulative probability plot for observed and simulated water depths for summer 2005, calibration (a) and summer 2007, validation (b).

increased roughness due to vegetation thus decreases during high flow events due to the water flow pressing down the water plants. As indicated in the methodology section, it is not possible to account for this effect directly in the MIKE11 software. Indirectly, however, this effect can be taken into account by relating the time-varying Manning's n to the magnitude of the rainfall runoff flow which then serves as an indicator of the river flow magnitude. The time-varying Manning's n then considers both the seasonal and flow-dependent changes. It was chosen to lower the Manning coefficient to 0.04 s $m^{-1/3}$ when the modelled rainfall runoff was larger than 3.5 m^3 s^{-1} because previous studies suggest that during high flow conditions, the Manning coefficients lower to almost the base Manning coefficient, that is, when there is no vegetation present (Whitehead *et al*. 1992; De Donker *et al.* 2011). This intervention increases the NSE from 0.65 for 2007 to 0.71, showing the importance to take into account this dependency.

The calibration procedure applied to determine the seasonally varying Manning coefficient obviously has been influenced by these peak flows. However, only 12 out of the 193 n values after calibration, which were used to fit the linear piecewise relationship, are affected by summer peak flows as defined by a rainfall runoff larger than 3.5 m^3 s^{-1}. Since these values do not show systematic deviations from the linear piecewise relation, there was no need to repeat the calibration taking into account deflection by peak flows.

By means of simulations with the hydrodynamic model, the impact of a changing roughness coefficient on the river

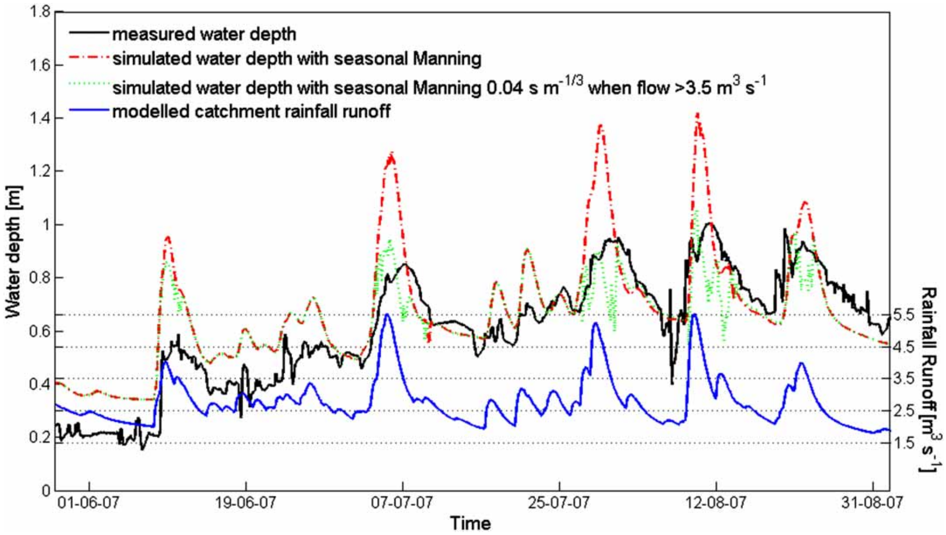

Figure 6 Observed versus MIKE11 simulated water depths, after use of a time-varying and flow-dependent Manning coefficient for summer 2007.

water levels was investigated (Figure 7). The corresponding Q–h curves with parameters that depend on the seasonal Manning's n, can be applied to estimate river discharges from measured water levels (Figure 8). When comparing the estimated discharge with the precipitation time series, it is clear that the estimation method based on the time-varying Q–h relation shows a better recession during dry periods compared with using a fixed rating curve. During long dry periods, indeed, exponentially recessive river flows are expected, $Q(t) = Q(t-1) \cdot exp\left(-1/k_{\mathrm{BF}}\right)$ where the baseflow recession constant k_{BF} is approximately constant for a given catchment or river location (Willems 2014).

4.2 *InfoWorks RS time-varying roughness coefficient*

Given that many results/dependencies obtained in Section 4.1 are based on MIKE11 model simulations, this section studies how these results depend on the hydrodynamic modelling software selected. The temporal variation of the Manning coefficient due to vegetation growth is modelled in InfoWorks RS with the RANS equation to estimate conveyance (Eq. 6). The calibration results based on the MIKE11 model show that the vegetation growth gives rise to the time-varying Manning coefficient in the period May–October and a constant one during the rest of the year. The Manning coefficient reaches a peak value in the middle of August and its lowest value in the

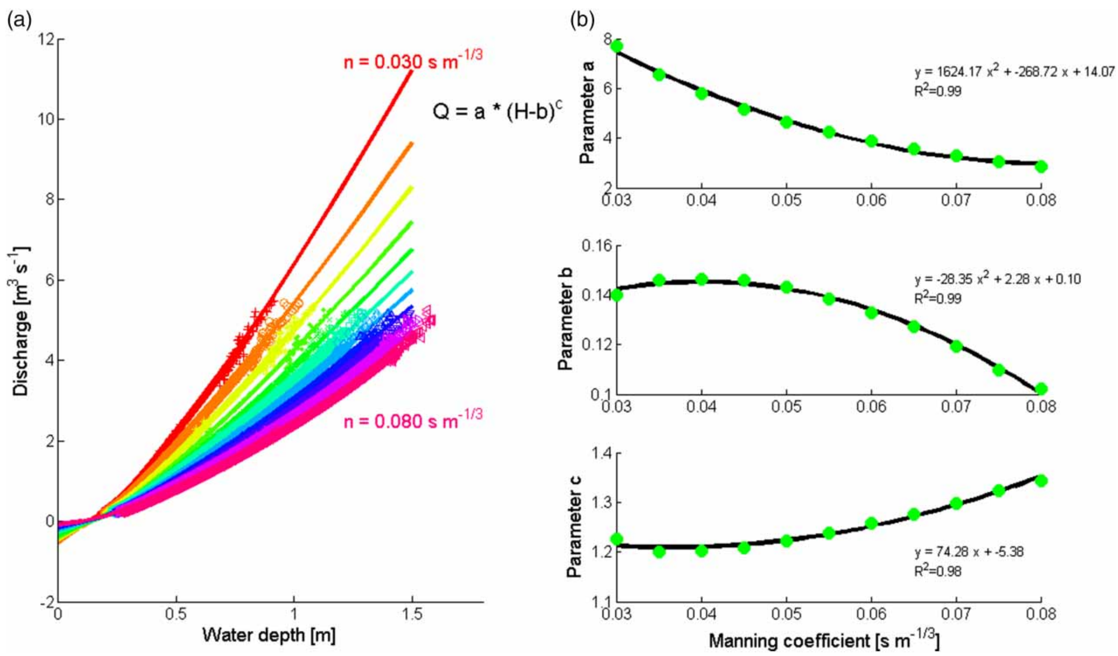

Figure 7 Rating curves for Manning coefficients ranging from 0.03 to 0.08 s m$^{-1/3}$ with an 0.005 interval (a) and relation of the rating curve parameters on the seasonal Manning coefficient (b).

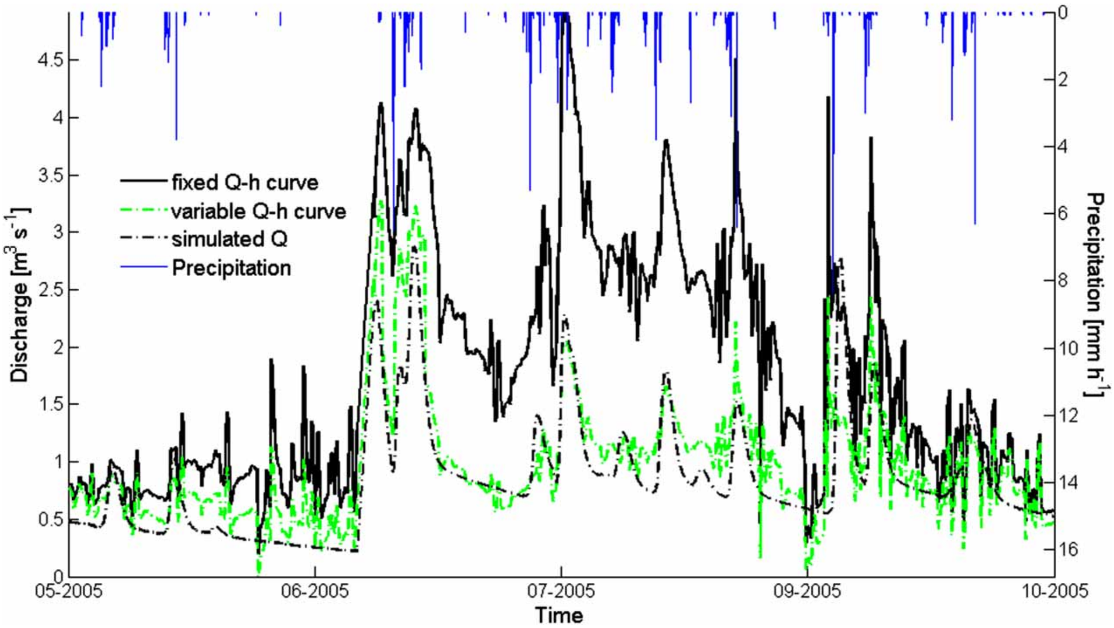

Figure 8 Comparison of the estimated river discharges, after use of a fixed and time-varying Q–h relationship with the MIKE11 simulated discharges and the precipitation time series for summer 2005.

constant period. The Manning coefficient is implemented in InfoWorks RS and calibrated to the MIKE11 simulation results by changing the maximum and minimum values determining the piecewise linear Manning's n relation. The calibrated minimum Manning coefficient is 7% lower in InfoWorks RS as compared with MIKE11 and the calibrated maximum Manning coefficient is 28% lower.

After calibration and validation of this time-varying Manning coefficient in the InfoWorks RS model, water level results match very well the MIKE11 results with NSE values of 0.991 and 0.988, respectively. However, the highest water levels in summer in both calibration and validation periods show noticeable differences. The largest difference is 0.028 m (which corresponds to 4.7% of the water depth) in the calibration period and 0.075 m

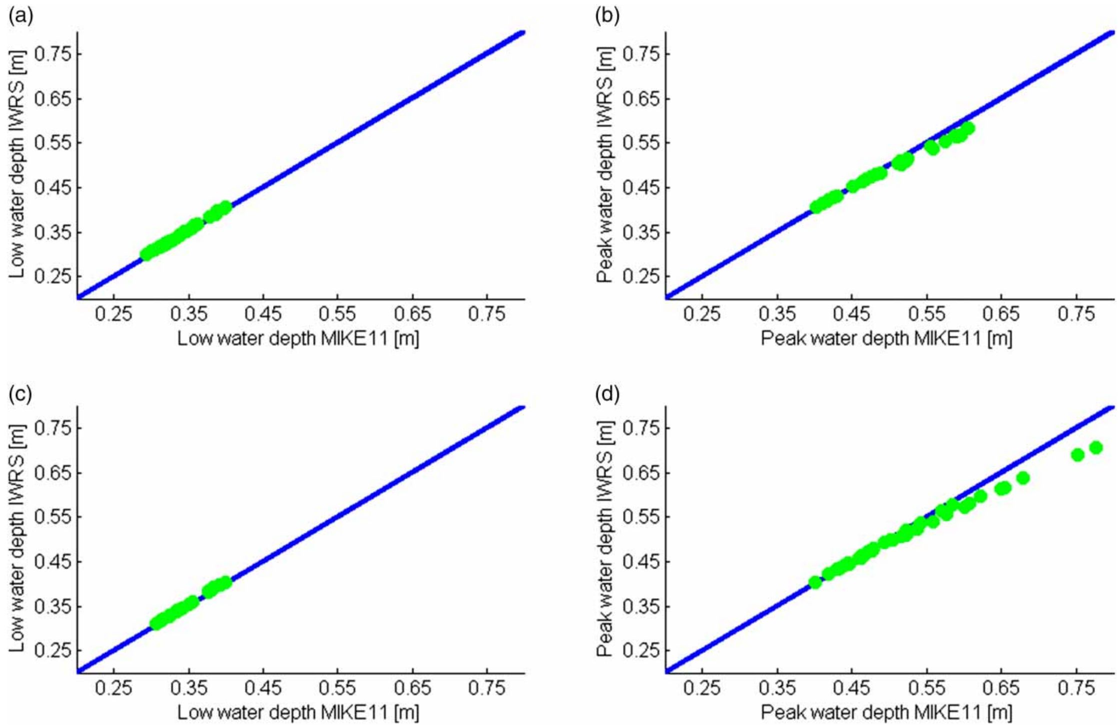

Figure 9 Correlation between independent water depths in MIKE11 and InfoWorks RS; for low (a) and peak (b) water depths in calibration period (2004–2005) and for low (c) and peak (d) water depths in validation period (2006–2007); at 8.034 km along the Molse Neet River.

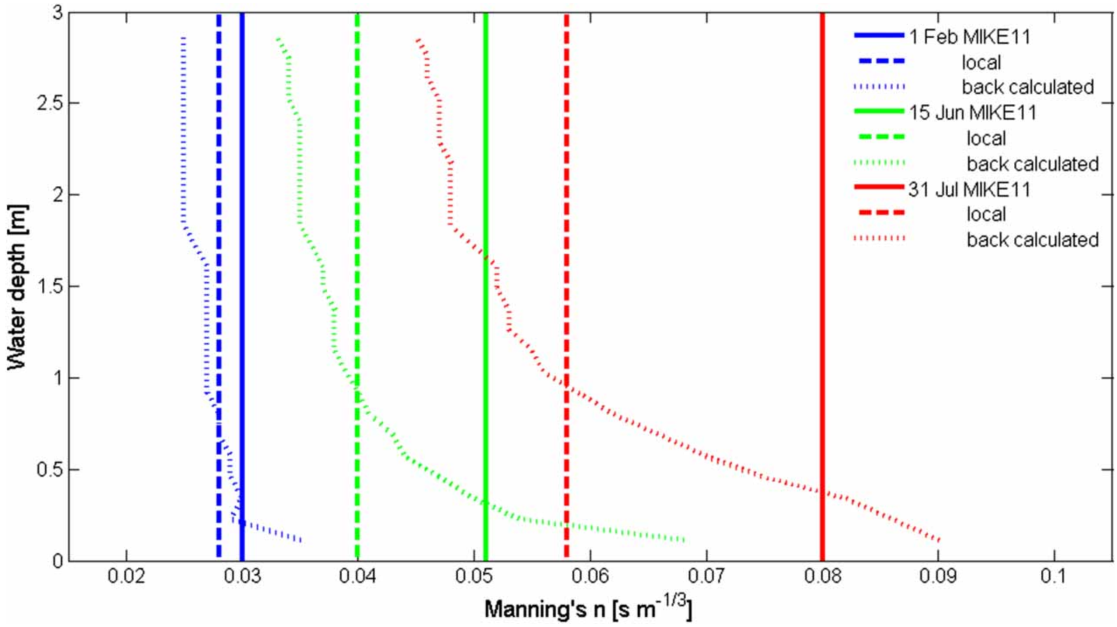

Figure 10 Local roughness, overall cross-section Manning's n in InfoWorks RS and MIKE11 at 8.034 km along the Molse Neet River on three specific days: 1 February, 15 June and 31 July.

(or 9.3% of the water depth) in the validation period. After extraction of independent peak and low flow water depths from the full simulation series, applying the method of Willems (2009), Figure 9 shows the comparison of these peak and low depths for the two models in calibration and validation periods. The results in both periods show that while the low water depths in InfoWorks RS are close to the ones in MIKE11 without systematic deviations, the peak water depths in InfoWorks RS are systematically lower than the MIKE11 results, with stronger differences for the higher water depths. The latter differences range from 0.04% for a water depth of 0.469 m to 4.69% for a water depth of 0.568 m in the calibration period, and from 0.04% difference for 0.477 m to 9.18% for 0.777 m in the validation period.

The systematic differences in peak water depths can be explained by the method of estimating the conveyance or the role of the Manning coefficient in the two models. Figure 10 shows the variation of local roughness, overall cross-section Manning's n in InfoWorks RS and MIKE11 as a function of water depth on three specific days of the year. In InfoWorks RS, the water depth increases while the overall cross-section Manning's n decreases, whereas in MIKE11, Manning's n remains constant at different water depths and there is no such reduction in water depth. Since the RANS model in InfoWorks RS considers the lateral shear, secondary flow and sinuosity, the overall cross-section Manning's n decreases in that model when the water depth increases. At very low water depth (i.e. 0.115 m), the overall cross-section Manning's n is larger than the local roughness. When the water depth increases, it decreases to the value of the local roughness at a certain depth, namely the transition point. The flow resistance is generated by the bed friction at the transition points only. After that, it rapidly decreases to smaller values.

Table 1 Transition depth in function of the total unit roughness

n_l (s m$^{-1/3}$)	Transition depth (m)
0.028	0.2
0.040	0.3
0.058	0.4

Furthermore, when the water depth increases, the overall cross-section Manning's n in InfoWorks RS decreases to Manning's n in MIKE11 at a transition depth. After that, it continues to decrease with deviation increasing with water depth. At the transition depth, simulated water depth in InfoWorks RS equals the one in MIKE11. These variations result in larger water depths for lower flows and lower water depths for larger flows. Additionally, the smaller local roughness has smaller transition depth (Table 1). This means that with lower local roughness, there are more simulated water depths in InfoWorks RS smaller than in MIKE11. However, at the same time, the discrepancies are smaller corresponding to lower deviation of Manning's n.

5 Conclusions and recommendations

In this study, the importance of a time-varying roughness coefficient for the accurate simulation of the water depths in full hydrodynamic river models has been shown. An increase in NSE from 0.33 to 0.67 can be obtained after applying a calibrated time-varying Manning coefficient. Implementation of the time-varying roughness coefficients in different hydrodynamic modelling systems can, however, lead to different results as is shown in this article after comparing MIKE11 and InfoWorks RS. The differences are due to different methods to estimate conveyance. Since considering different energy losses due to bed friction, lateral flow, secondary flow and sinuosity, InfoWorks RS can simulate the reduction of overall cross-section Manning's *n* in water depth. This results in lower water depths at high flows and larger water depths at low flows in InfoWorks RS in comparison with MIKE11. However, in general, the simulated water depths show that the difference in implicit scheme to solve the Saint Venant equations and methods to estimate conveyance does not significantly influence the simulation results (relative water depth differences less than 10%). MIKE11 and InfoWorks RS thus have an equivalent capacity to model vegetation growth, or, more in general, variation of roughness. These conclusions are based on simulation results for four years without the inclusion of flood branches. InfoWorks RS can model secondary flows due to flooding through the RANS model, whereas this effect cannot be incorporated into the empirical Manning equation. We therefore recommend extending this analysis for both inbank and overbanking flow in inundation events and based on water level measurements at more locations.

The analysis also confirms that although the roughness increases during the summer due to plant growth, the roughness is diminished again during periods of peak flows. It is thus important to take into account the seasonally changing roughness coefficient when the hydrodynamic model is coupled to a water quality model. Water quality concentrations are indeed highly influenced by the river water velocity. However, when studying river floods, that is, there is only an interest in high peak flows, it might be acceptable to work with a constant roughness coefficient.

The article finally has shown how hydrodynamic models can be used to establish adjusted rating curves for the summer months as the Q–h relationship may not remain constant in time due to vegetation change; strong changes were shown in this study for the Meerhout station. Not updating the rating curves seasonally can lead to overestimations of the observed water level-based discharge estimates, by more than 100% for specific locations in this case study.

Acknowledgements

The Province of Antwerp and the Flemish Environment Agency (VMM) are gratefully acknowledged for providing the measurement data on cross-sections and structures along the rivers in the Grote Nete catchment; the Hydraulic Information Centre (HIC) for the provision of the water height measurements and the derived discharge estimates. Finally, DHI Water & Environment and Innovyze are respectively acknowledged for the provision of the license for the MIKE11 and InfoWorks RS software.

Funding

This research has been supported by a Ph.D. fellowship grant of the Research Foundation – Flanders (FWO) to the first author and an IRO scholarship to the second author.

ORCID

Ingrid Keupers http://orcid.org/0000-0001-5844-5860
Thuy Nguyen Thanh http://orcid.org/0000-0003-0546-6603
Patrick Willems http://orcid.org/0000-0002-7085-2570

References

Abbott, M. and Ionescu, F., 1967. On the numerical computation of nearly-horizontal flows. *Journal of Hydraulics Research*, 5, 97–117. doi:10.1080/00221686709500195

Abril, B., 2003. *Benchmark comparisons of the analytical and finite element solutions of the SKM*. UK: University of Birmingham, Technical Report EPSRC Research Grant – GR/R54880/01.

Anderson, B.G., Rutherfurd, I.D., and Western, A.W., 2006. An analysis of the influence of riparian vegetation on the propagation of flood waves. *Environmental Modelling & Software*, 21 (9), 1290–1296. doi:10.1016/j.envsoft.2005.04.027

Arcement, G. and Schneider, V., 1984. Guide for selecting Manning's roughness coefficients for natural channels and flood plains. [FHWA-TS-84-204]. Washington, DC: Federal Highway Administration.

Aricò, C., Nasello, C., and Tucciarelli, T., 2009. Using unsteady-state water level data to estimate channel roughness and discharge hydrograph. *Advances in Water Resources*, 32 (8), 1223–1240.

Aricò, C., *et al.*, 2010. Discharge estimation in open channels by means of water level hydrograph analysis. *Journal of Hydraulic Research*, 48 (5), 612–619. doi:10.1080/00221686.2010.507352

Aronica, G., Hankin, B., and Beven, K., 1998. Uncertainty and equifinality in calibrating distributed roughness coefficients in a flood propagation model with limited data. *Advances in Water Resources*, 22 (4), 349–365. doi:10.1016/S0309-1708(98)00017-7

Bakry, M.F., Gates, T.K., and Khattab, A.F., 1992. Field-measured hydraulic resistance characteristics in vegetation-infested canals. *Journal of Irrigation and Drainage Engineering*, 118 (2), 256–274. doi:10.1061/(ASCE)0733-9437(1992)118:2(256)

Barnett, A. and Shamseldin, A., 2009. *Hydraulic effects of Riparian Plantings*. [TR 2009/096]. Auckland: Auckland Regional Council.

De Doncker, L., *et al.*, 2011. Deriving the relationship among discharge, biomass and Manning's coefficient through a calibration approach. *Hydrological Processes*, 25 (12), 1979–1995. doi:10.1002/hyp.7978

DEFRA/EA, 2002. Reduce Uncertainty in River Flood Conveyance. Interim Report 2: Review of methods for Estimating Conveyance. [W5A - 057]. Bristol, UK: Environment Agency.

DHI, 2011. *MIKE11 reference manual*. Hørsholm, Denmark: DHI Water & Environment.

Ervine, D.A., Babaeyan-Koopaei, K., and Sellin, H.J., 2000. Two-dimensional solution for straight and meandering

overbank flows. *Journal of Hydraulic Engineering*, 126 (9), 653–669. doi:10.1061/(ASCE)0733-9429(2000)126:9(653)
Gurnell, A.M. and Midgley, P., 1994. Aquatic weed growth and flow resistance – influence on the relationship between discharge and stage over a 25 year river gauging station record. *Hydrological Processes*, 8 (1), 63–73. doi:10.1002/hyp.3360080105
Green, J.C., 2005. Modelling flow resistance in vegetated streams: review and development of new theory. *Hydrological Processes*, 19 (6), 1245–1259. doi:10.1002/hyp.5564
Green, J.C., 2006. Effect of macrophyte spatial variability on channel resistance. *Advances in Water Resources*, 29 (3), 426–438. doi:10.1016/j.advwatres.2005.05.010
Järvelä, J., 2002. Flow resistance of flexible and stiff vegetation: a flume study with natural plants. *Journal of Hydrology*, 269 (1–2), 44–54. doi:10.1016/S0022-1694(02)00193-2
Keupers, I. and Willems, P., 2013. Impact of urban WWTP and CSO fluxes on river peak flow extremes under current and future climate conditions. *Water Science and Technology*, 67 (12), 2670–2676. doi:10.2166/wst.2013.147
King, A.M., 2011. Effects of Aquatic Macrophyte Cover on Bed Roughness in the Shasta River, California. Thesis (PhD). University of California.
Nash, J.E. and Sutcliffe, J.V., 1970. River flow forecasting through conceptual models. Part I: a discussion of principles. *Journal of Hydrology*, 10 (3), 282–290.
Pham, N., *et al*., 2011. Effects of submerged tropical macrophytes on flow resistance and velocity profiles in open channels. *International Journal of River Basin Management*, 9, 195–203. doi:10.1080/15715124.2011.648775
Preissmann, A., 1961. Propagation des intumescences dans les canaux et rivières. Presented at the 1st Congress of the French Association for Computation, Grenoble, France, 1961.
Schulz, M., *et al*., 2003. The influence of macrophytes on sedimentation and nutrient retention in the lower River Spree (Germany). *Water Research*, 37 (3), 569–578. doi:10.1016/S0043-1354(02)00276-2
Straatsma, M.W., *et al*., 2013. Uncertainty in hydromorphological and ecological modelling of lowland river floodplains resulting from land cover classification errors. *Environmental Modelling & Software*, 42, 17–29. doi:10.1016/j.envsoft.2012.11.014
Vansteenkiste, T., *et al*., 2014. Intercomparison of climate scenario impact predictions by a lumped and distributed model ensemble. *Journal of Hydrology*, 511, 335–349. doi:10.1016/j.jhydrol.2014.01.050
Watson, D., 1987. Hydraulic effects of aquatic weeds in UK rivers. *Regulated Rivers: Research & Management*, 1, 211–227. doi:10.1002/rrr.3450010303
Whitehead, E., Brown, P., and Hollinrake, P., 1992. *The hydraulic resistance of vegetated channels*. [Report SR 305]. Oxfordshire, UK: HR Wallingford.
Wijns, K. and Wilkin, N., 2007. Hydrologische en hydraulische studie van het stroomgebied van de waterlopen Mol Neet, Scheppelijke Neet en Oude Neet van tweede categorie Deelrapport 1: Inventarisatie en hydrologie van het stroomgebied van de Mol Neet, Scheppelijke Neet en Oude Neet. Mechelen, Belgium: Haskoning, 816747/R/kw/Mech. [in Dutch].
Willems, P., 2009. A time series tool to support the multi-criteria performance evaluation of rainfall-runoff models. *Environmental Modelling & Software*, 24 (3), 311–321. doi:10.1016/j.envsoft.2008.09.005
Willems, P., 2014. Parsimonious rainfall-runoff model construction supported by time series processing and validation of hydrological extremes – part 1: step-wise model-structure identification and calibration approach. *Journal of Hydrology*, 510, 578–590. doi:10.1016/j.jhydrol.2014.01.017
Wilson, C., 2007. Flow resistance models for flexible submerged vegetation. *Journal of Hydrology*, 342 (3–4), 213–222. doi:10.1016/j.jhydrol.2007.04.022
Woldeamlak, S., Batelaan, O., and De Smedt, F., 2007. Effects of climate change on the groundwater system in the Grote-Nete catchment, Belgium. *Hydrogeology Journal*, 15, 891–90. doi:10.1007/s10040-006-0145-x